

**DAMPING BEHAVIOUR OF FLEXIBLE LAMINATES**

by

**V.A. Coveney, A.H. Muhr & A.G. Thomas**

Malaysian Rubber Producers' Research Association  
Tun Abdul Razak Laboratory  
Brickendonbury,  
Hertford SG13 8NL  
England

**ABSTRACT**

Formulae for the mechanics of flexing of laminates of a viscoelastic material, such as an elastomer, and an inextensible material, such as steel, have been derived and compared to experiment. In particular, equations for the profile, stiffness and partition of energy between elastomer and metal are given.

The effect of an axial load on the lateral stiffness of laminar struts is investigated both theoretically and in experiments on free oscillation. As the axial load approaches the buckling load, the apparent damping level to lateral oscillations becomes very large. Conversely for an axial tension the lateral stiffness is enhanced and the damping to lateral oscillations is diminished. Other examples of this phenomenon, which is not peculiar to the laminates, are given.

## 1. INTRODUCTION

A characteristic of rubber springs is that they have relatively high damping, and within limits the rubber compound can be chosen to give the required level of damping. Each type of conventional rubber spring has a characteristic force-deformation behaviour which may be convenient for a particular application. In this work the properties of an unconventional rubber spring will be described, which lends itself to control of the damping level, and may have other advantages for some applications. The spring consists of a sandwich structure of metal and rubber (Figure 1). Attention will be concentrated on the flexing mode of deformation (analogous to that of a leaf spring).

The mathematical expressions for the mechanical properties of the laminate are relatively simple, so the properties can be readily calculated. While this is a desirable state of affairs for an engineering component, it also means that physical insight is not obscured by mathematical complexity. For example, not only is the effect of an axial load on the stability and apparent damping level (to lateral oscillations) easy to investigate for the laminates, but the effect also helps provide insight into a general phenomenon.

## 2. MECHANICS OF FLEXING OF RUBBER-STEEL LAMINATES

It is assumed that:

- (i) there is no strain normal to the plane of flexure (so all forces etc. will be taken per unit breadth of laminate)
- (ii) the rubber is incompressible.

### Thin, inextensible metal layers

Then, if the further assumption is made that the metal layers are inextensible and much thinner than the rubber layers ( $t \ll h$ ), it follows that the state of deformation of the rubber is simple shear and the metal layers deform to have a common centre of curvature. This is demonstrated in Figure 2, from which it may be readily concluded that the volume of the element PQRS is constant provided:

$$\delta v = h\delta\theta \quad (1)$$

which is the condition of inextensibility.

Since the element PQRS is not necessarily initially in a state of zero shear,  $\delta v$  may be identified with the increase in shear movement of one metal layer relative to the other. Thus the angle of shear  $\gamma$  is related to the slope  $\theta$  of the laminate by:

$$d(\tan\gamma)/d\theta = 1 \quad (2)$$

Equation (2) may be integrated and for the case that the deflection  $y$  of the laminate is small so that all the angles are small, simplified to give:

$$\tan \gamma = \theta + \text{constant} = dy/dx + \text{constant} \quad (3)$$

where the co-ordinates  $(x,y)$  are defined in Figure 2. Throughout the rest of this paper the choice of co-ordinates allows the constant term in (3) to be dropped, since it can in each case be seen that  $\tan \gamma = 0$  when  $dy/dx = 0$ . Only in relating  $\theta$  to  $dy/dx$  has the assumption of small angles (and hence large radius of curvature of the laminate and small strain in the rubber) been made, equations (1) and (2) being of more general validity.

The shear in an element of rubber imposes an increment  $\delta F$  in compressive force per unit breadth on one metal layer and a corresponding increment in tensile force on the other layer:

$$\delta F = G \delta x \cdot \tan \gamma \quad (4)$$

where  $G$  is the shear modulus of the rubber. Integration of equation (4), using appropriate boundary conditions, yields the compressive (or tensile) force  $F$  as a function of  $x$ .

The differential equation describing the profile of the flexed laminate can be derived by consideration of the forces on an element, as depicted in Figure 3. The total shear force  $S$  per unit breadth borne by the laminate is distributed between the shear force  $S_R$  borne by the rubber layer and the shear forces  $S_1$  and  $S_2$  borne by the metal layers.

$$S = S_1 + S_2 + S_R \quad (5)$$

Relating  $S_R$  to the shear in the rubber and  $S_1$  and  $S_2$  to the curvature gradient in the metal ( $S_1 = -dM_1/dx$ ,  $S_2 = -dM_2/dx$ , where  $M_1$  and  $M_2$  are the bending moments in the metal layers), equation (5) can be written as

$$\begin{aligned} S &= G \tan \gamma - d(M_1 + M_2)/dx \\ &= G \tan \gamma - K(d^3 y/dx^3) \end{aligned} \quad (6)$$

where it has been assumed that the radius of curvature is large compared to the laminate thickness and  $K$  is given by

$$K = k_1 + k_2 = (E_1 t_1^3 + E_2 t_2^3)/12 \quad (7)$$

where  $k_1$ ,  $k_2$  are the bending stiffnesses of the metal layers,  $E_1$ ,  $E_2$  are their Young's moduli and  $t_1$ ,  $t_2$  are their thicknesses (in the rest of this paper  $E_1 = E_2$ ,  $t_1 = t_2$  so that the subscripts will be dropped). Inserting (3) into (6) gives

$$S = Gh(dy/dx) - K(d^3 y/dx^3) \quad (8)$$

which is applicable for the case that  $t \ll h$  and the metal layers are inextensible.

The local strain energy density in the rubber is just  $0.5G(\tan\gamma)^2$  so that the total strain energy (per unit width)  $U_R$  stored in the rubber is

$$U_R = 0.5Gh \int (dy/dx)^2 dx \quad (9)$$

where use has been made of equation (3).

The energy stored in the metal layers can similarly be calculated as

$$U_M = 0.5K \int (d^2y/dx^2)^2 dx \quad (10)$$

The total energy stored is  $U_R + U_M$

#### Geometric effect of thick metal layers

If the metal layers have an appreciable thickness the assumption that  $t \ll h$  must be relaxed. However, to a small angle approximation assumptions (i) and (ii) are satisfied if the deformation is such that the central lines of the metal layers have a common centre of curvature. The rubber is not then just deformed in simple shear but suffers some compression and extension on the surfaces bonded to the metal in regions of curvature. However, the effect is still an increment  $\delta v$  to the shear movement, given this time by:

$$\delta v = (h + (t_1 + t_2)/2) \delta \theta \quad (11)$$

Thus equation (3) becomes:

$$\tan\gamma = \frac{2h + t_1 + t_2}{2h} (dy/dx)$$

A further modification required for thick metal layers is that the shear stress in the laminate falls from  $G \tan\gamma$  in the rubber to zero across the thickness of the metal layers, so that the shear term  $S_R$  in equation (5) becomes:

$$S_R = G \tan\gamma (h + (t_1 + t_2)/2)$$

Thus equation (8) becomes:

$$S = G \frac{(2h + t_1 + t_2)^2}{4h} \frac{dy}{dx} - K \frac{d^3y}{dx^3} \quad (12)$$

Equation (12) has the same form as equation (8) but the geometric effect of the thick metal layers enhances the magnitude of the shear term from the rubber core. Hence in most of the work below the results are derived from (8), but the results are valid for thicker metal layers provided  $Gh$  is replaced by  $G(2h + t_1 + t_2)^2/4h$ .

Effect of extension of the metal layers

Under the actions of the forces given by equation (4) the metal layers will suffer some longitudinal extension. The neutral axes will no longer coincide with the centre lines, and equations (1) and (11) will not be accurate. Mead and Markus<sup>1</sup> have allowed for this effect by means of an additional term involving the longitudinal extensions. This leads to an additional differential equation to their analogue of equation (8) or (12). Elimination of the longitudinal extensions from the pair of differential equations yields a fifth order differential equation analogous to (8) or (12).

This complication is not addressed in our work. As a consequence, the limits as  $h \rightarrow 0$  (but  $G$  is kept fixed) correspond to metal layers which are allowed to slip at the interface, instead of metal layers which are bonded at the interface (which then becomes the common neutral axis). Thus there is an implicit assumption that as  $h$  is reduced to zero, so  $G$  is reduced to zero. A criterion for the validity of our equations is derived below.

3. THREE-POINT BEND GEOMETRYProfile

The three point bend geometry, shown in Figure 4, is a convenient deformation for experimental measurement of the dynamic properties of the laminate on a servohydraulic test machine. It is necessary to treat the laminate in two parts,  $0 < x < \ell$  which covers the central region, and  $-a < x < 0$  which covers the overhanging region. It can be shown that in the two extreme cases of  $G=0$  and of  $K=0$  that the overhanging region does not influence the force-deflection behaviour, but it does have to be considered in the general case.

The profile will be symmetrical about  $x=\ell$ , so it is only necessary to solve the problem for  $x < \ell$ .

Considering first the portion of the laminate for  $0 < x < \ell$ , the bending moment  $B$  exerted on a portion of laminate to the left of the point  $(x,y)$  is given by

$$B = -Wx \quad (13)$$

$B$  is related to the shear force  $S$  in the beam by

$$S = -dB/dx \quad (14)$$

inserting (14) into equation (8), and making use of (13) gives

$$W = Gh(dy/dx) - K(d^3y/dx^3) \quad (15)$$

The differential equation describing the profile in the region  $-a < x < 0$  is the same as (15) but with  $W$  set to zero.

These differential equations are required to be solved subject to the boundary conditions

- (i) at  $x = -a$ ,  $d^2y/dx^2 = 0$  since the bending moment in the metal here must be zero as it is a free end
- (ii) at  $x = 0$ ,  $y = 0$  while  $dy/dx$  and  $d^2y/dx^2$  must be the same for both equations
- (iii) at  $x = \ell$ ,  $dy/dx = 0$  as required by symmetry.

The solutions are

$$\text{for } -a < x < 0, \quad y = A_2 (e^{\alpha x} - 1) + B_2 (e^{-\alpha x} - 1)$$

$$\text{for } 0 < x < \ell \quad y = A_1 (e^{\alpha x} - 1) + B_1 (e^{-\alpha x} - 1) + Wx/Gh$$

$$\text{where } \alpha^2 = Gh/K$$

$$A_1 = (W/\alpha Gh) \frac{q^2 - 1 - 2pq^2}{2(1 + p^2q^2)} \quad (16)$$

$$A_2 = A_1 + (W/2\alpha Gh)$$

$$B_1 = p(A_1 p + W/\alpha Gh)$$

$$B_2 = -A_2/q^2$$

$$p = e^{\alpha \ell}, \quad q = e^{\alpha a}$$

It has been reported previously<sup>2</sup> that equation (16) is in good agreement with experimental observation of the profile. The deflection  $Y$  at  $x = \ell$  can be found from (16) and this leads to an expression for the stiffness of the laminate in the 3-point bend geometry:

$$(2W/Y)(\ell/2Gh) = \frac{2\alpha\ell(1+p^2q^2)}{2\alpha\ell(1+p^2q^2) + (1-p)(3-q^2-p+3pq^2)} \quad (17)$$

The quantity  $\ell/2Gh$  represents the compliance in the limit of  $\alpha\ell \rightarrow \infty$ , and is equal to that of a rubber spring undergoing simple shear. The quantity  $\alpha\ell$  is a non-dimensional measure of the relative importance of rubber and metal, and it is convenient to express all the results as functions of  $\alpha\ell$  (as in equation (17)).

Stored energy in 3-point bend

Inserting equation (16) into the integral expression (9) the energy stored in the rubber is given by

$$\begin{aligned}
 U_{R1} \text{ overhang} &= \frac{Gh}{2} \int_{-a}^0 (dy/dx)^2 dx \\
 &= \frac{Gh\alpha}{4} \{A_2^2(1-1/q^2) - B_2^2(1-q^2) - 4\alpha a A_2 B_2\} \quad (18)
 \end{aligned}$$

$$\begin{aligned}
 U_{R2} \text{ central section} &= \frac{Gh}{2} \int_0^l (dy/dx)^2 dx \\
 &= \frac{Gh\alpha}{4} \{A_1^2(p^2-1) - B_1^2(1/p^2-1) - 4\alpha l A_1 B_1 \\
 &\quad + 2(W/Gh)^2 \alpha / \alpha + (4W/\alpha Gh)(A_1 p + B_1/p - A_1 - B_1)\} \quad (19)
 \end{aligned}$$

Since the energy loss associated with deforming rubber (per unit of stored energy) greatly exceeds that of metals (for strains below the yield point) the energy loss associated with deforming the laminate will be proportional to  $U_R = U_{R1} + U_{R2}$ . A plot of  $U_R/(U_R + U_M)$  versus  $\alpha l$  is given in Figure 5 with values of  $a/l$  as a parameter. It is apparent that that the overhang region ( $-a < x < 0$ ) only makes an appreciable difference for values of  $\alpha l$  such that the total energy is fairly evenly partitioned between rubber and metal. This effect is investigated further in Figure 6 where  $U_{R1}/(U_R + U_M)$  is plotted against  $\alpha l$  with  $a/l$  as a parameter. At small values of  $\alpha l$  the simple theory predicts a significant fraction of the deformation energy to be stored in the rubber in the overhang region. This is a manifestation of the effect of a constrained layer on the damping of panels since it suggests that a constrained layer covering a large region of a panel will have a useful damping effect on a local deformation.

Forces in the metal layers

It follows from equations (4) and (11), and from the fact that the axial force in the metal layer at  $x = -a$  is zero, that the compressive force per unit width in the top metal layer is

$$F = G \frac{2h+t_1+t_2}{2h} (y - Y_a) \quad (20)$$

where  $Y_a = y(x = -a)$ .

It is apparent from (20) that  $F$  rises to a maximum value of  $F=G(Y+Y_a)$  at  $x=l$ . If this maximum value is sufficiently large the metal layer can buckle in a manner similar to an Eulerian strut, (although the constraint of bonding to the rubber must be taken into account<sup>2</sup>). This has the effect of limiting the permissible deflection  $Y$ .

The force in the bottom metal layer will, according to the boundary condition, be equal and opposite to that in the top layer. A further significance of these forces is that the resultant strain in the metal layers may lead to a departure from the assumption of inextensibility which was used to derive equation (1).

The condition of inextensibility of the metal layers may be expressed as

$$\int \epsilon \, dx \ll 0.5 v_{\max} = 0.5(h+(t_1+t_2)/2)(dy/dx)_{\max} \quad (21)$$

where the left hand side is the change in length of one metal layer due to its axial strain and the right hand side is the shear displacement predicted by equation (11) (reduced by a factor of one half since it is 'shared' between the metal layers). The axial strain  $\epsilon$  is just  $F/Et$ , which using (20) gives

$$\epsilon = \frac{G}{Et} \frac{(2h+t_1+t_2)}{2h} (Y-Y_a) \quad (22)$$

For the extreme case of large  $\alpha l$ ,  $y=(x/l)Y$  (with  $y=0$  in the overhang) so that (21) becomes

$$G/E \ll ht/\alpha^2 \quad (23)$$

while for the extreme case that  $\alpha l$  is small,  $y=(W/2K)(\alpha^2 x-x^3/3)$  (with  $dy/dx$  constant in the overhang) so that (21) can be recast as

$$G/E \ll ht/(\alpha^2 l^2 a + 5\alpha^2/6) \quad (24)$$

For rubber  $G \sim 1\text{MPa}$  while for steel  $E = 210\text{GPa}$ , so the left hand side of (23) or (24) is about  $5 \times 10^{-7}$ . This means that provided the length to thickness ratio of the laminate is less than 100, a ratio of up to 100 between  $t$  and  $h$  is allowable. Thus for the system studied here equations (8) or (12) have a very broad range of validity. They may also be applicable to many cases of composite beams with a core layer of viscoelastic material other than rubber.

#### 4. LAMINAR STRUTS SUBJECTED TO AN AXIAL FORCE

##### Profile

Interconnecting the metal layers of the laminate depicted in Figure 7 leads to the following boundary conditions:

$$\left. \begin{array}{l} \text{at } x=0 \quad y=0 \\ \text{at } x=0, l \quad dy/dx=0 \end{array} \right\} \quad (25)$$



where the second condition expresses the fact that the radius of curvature of the metal layer is finite.

The total bending moment  $B$  applied by the laminate on the right hand side of position  $x$  to the laminate on the left hand side is

$$B = M+W(\ell-x) + P(Y-y) \quad (26)$$

where  $Y$  is the deflection at  $y=\ell$ .

Proceeding as for the three-point bend geometry then leads to

$$W = (Gh-P)dy/dx - K(d^3y/dx^3) \quad (27)$$

Integrating the equation once gives

$$d^2y/dx^2 - \alpha^2y = -Wx/K + C \quad (28)$$

where  $\alpha^2 = (Gh-P)/K$

Since  $\alpha$  is imaginary for  $P > Gh$  it is convenient to express the solution of (28) in hyperbolic functions rather than exponentials:

$$y = A\sinh\alpha x + B\cosh\alpha x - \frac{Wx}{K\alpha^2} + \frac{C}{\alpha^2} \quad (29)$$

Using the boundary conditions (25) to find values for the integration constants  $A$ ,  $B$  and  $C$  gives

$$y = W/K\alpha^3 [p\cosh\alpha x - \sinh\alpha x + \alpha x - p] \quad \}$$

where  $\alpha^2 = (Gh-P)/K \quad \}$  (30)

$$p = \tanh(\alpha\ell/2) \quad \}$$

### Stiffness

The stiffness  $W/Y$  may be found from (30) by setting  $x=\ell$ . Algebraic simplification then leads to

$$\frac{W}{Y} = \frac{Gh}{\ell} \left(1 - \frac{P}{Gh}\right) \left(\frac{\alpha\ell}{\alpha\ell - 2p}\right) \quad (31)$$

The quantity  $Gh/\ell$  has been isolated in equation (31) because it is the value that  $W/Y$  takes for zero  $P$  and infinite  $\alpha\ell$ , and is equivalent to a rubber simple shear spring. A plot of  $(W/Y)(\ell/Gh)$  for  $P=0$  versus  $\alpha\ell$  (where  $\alpha^2 = Gh/K$ ) is given in Figure 8.

The effect of  $P$  on the stiffness is of interest. When  $P > Gh$ , equation (31) becomes

$$\frac{W}{Y} = \frac{Gh}{\ell} \left( \frac{P}{Gh} - 1 \right) \left( \frac{\beta \ell}{2q - \beta \ell} \right) \quad (32)$$

$$\begin{aligned} \text{where } \beta^2 &= (P - Gh)/K \\ q &= \tan(\beta \ell / 2) \end{aligned}$$

Using equation (31) when  $P < Gh$  and equation (32) when  $P > Gh$ , the non-dimensional stiffness  $(W/Y)(\ell/Gh)$  can be plotted against the non-dimensional normal load  $P/Gh$ . The results are given in Figure 9, with  $\alpha_0 \ell$  as a parameter.

### Stability

As  $\beta \ell \rightarrow \pi$ ,  $q \rightarrow \infty$  so that, from equation (32), the stiffness falls to zero. This is the point of instability, and the stability criterion may be expressed as

$$\begin{aligned} \beta^* \ell &= \pi \\ P^* &= Gh(1 + (\pi/\alpha_0 \ell)^2) \end{aligned} \quad (33)$$

For  $Gh = 0$ , this reduces to the usual Eulerian buckling relation.

### Elastic energy stored in the flexed laminate

Equation (30) may be used to evaluate  $dy/dx$  and hence  $U_R$ , using equation (9). This gives

$$U_R = (GhW^2/2K^2\alpha^5) \{3\alpha\ell/2 - 3p - p^2\alpha\ell/2\} \quad (34)$$

Substituting for  $W^2$  using equation (31) gives

$$U_R/Y^2 = \frac{1}{2} \left( \frac{Gh}{\ell} \right) \cdot \frac{1}{\alpha\ell} \cdot \{3\alpha\ell/2 - 3p - p^2\alpha\ell/2\} \left( \frac{\alpha\ell}{\alpha\ell - 2p} \right)^2 \quad (35)$$

In the case the  $P > Gh$ , (35) becomes

$$U_R/Y^2 = \frac{1}{2} \left( \frac{Gh}{\ell} \right) \frac{1}{\beta\ell} \{3\beta\ell/2 - 3q + q^2\beta\ell/2\} \left( \frac{\beta\ell}{\beta\ell - 2q} \right)^2 \quad (36)$$

The term  $0.5(Gh/\ell)$  may be identified as the energy stored in a rubber simple shear spring at unit deflection (ie. the limit as  $\alpha_0 \ell \rightarrow \infty$ ). A plot of the non-dimensional energy  $U_R/(Y^2 Gh/2\ell)$  versus  $P/Gh^0$  is given in Figure 10 with  $\alpha_0 \ell$  as a parameter. For  $P/Gh=1$  the profile will be independent of  $\alpha_0 \ell$ , thus explaining why all the plots in the Figure coincide at that point, since the energy in the rubber ( $U_R$ ) depends on the profile. In all cases  $U_R$  exceeds the value for rubber in uniform simple shear ( $GhY^2/2\ell$ ). This is because the profile departs from a straight line configuration, for which the shear energy in the rubber is a minimum, when  $K$  is non zero.

It is also of interest to consider the ratio  $E_R$  of the energy stored in the rubber to the work done by the lateral force in deflecting the strut:

$$E_R = U_R / 0.5WY$$

A plot of  $E_R$  versus  $P/Gh$  is given in Figure 11 with  $\alpha_0$  as a parameter. The magnitude of  $E_R$  determines the degree of damping experienced by lateral oscillations, as discussed below.

### Forces in the metal layers

There are three contributions to the axial loading  $F$  in the metal - the imposed axial load  $P$ , the imposed moment  $M$  and the contributions  $\delta F$  from the shear in the rubber (equation (4)). This makes the domain of validity of the equations less broad than implied by equations (23) or (24). However, the values of  $P$  and  $M$  applied in the experiments were so modest as to not greatly affect the earlier conclusions regarding validity.

## 5. EXPERIMENTAL

Experimental checks of some aspects of the theory have been reported previously<sup>2,3</sup> and where appropriate these results have been entered as points on the diagrams, thus allowing comparison with the theory.

Of particular interest here are the experimental measurements of the fraction of energy stored in the rubber,  $U_R / (U_R + U_M)$  (Figure 5). The dynamic behaviour of the laminates was measured using a servohydraulic test machine. There were initial problems regarding the method of support of the laminate in three point bend configuration, since the metal layer tended to slide over the supports as the laminate was bent, causing frictional energy loss. This was overcome by bonding to the supports small resilient rubber pads which could deform very easily in shear, but themselves dissipate very little energy. In this manner a reliable measurement of the loss angle  $\delta_0$  of the laminate could be made. The fraction of deformation energy of the laminate stored in the rubber can be found from  $\delta_0$  and an independent measurement of the loss angle  $\delta_r$  of the rubber:

$$U_R / (U_R + U_M) = \sin \delta_0 / \sin \delta_r \quad (37)$$

where it has been assumed that the loss in the metal is negligible.

Further experimental work has now been undertaken to check the theory for the effect of axial load on the stiffness and damping of struts consisting of laminates with the metal layers interconnected at each end. These laminates were constructed by bonding (during vulcanization) nominal 0.25mm spring steel strips to each side of an unfilled natural

rubber compound. The spring steel layers were separated at each end by mild steel blocks, through which bolts passed which served as both a means of attaching the struts and to prevent relative shear displacements (at the ends of the strut) between the metal layers. The shear modulus of the rubber was measured using a separate testpiece (double shear) on a servohydraulic machine, giving a value of  $G = 0.52\text{MPa}$ . The logarithmic decrement of the rubber was determined from free torsional oscillation of the double shear testpiece at 9.3Hz. This gave a value of 0.0729, and there was very little frequency dependence. The pertinent laminate dimensions were  $\lambda = 257\text{mm}$  (measured from the inside edges of the mild steel end blocks), width of rubber = 44mm, width of spring steel = 57mm,  $K = 0.74\text{Nm}$  (calculated from the measured thickness of steel, 0.27mm, and adjusted according to the excess width of steel).

The axial load was applied by means of weights as depicted in Figure 12. The stiffness  $W/Y$  and damping of the combined laminates were calculated from the frequency  $f$  and logarithmic decrement  $\Lambda$  of the natural oscillations of the structure according to

$$W/Y = M(2\pi f)^2 \quad (38)$$

$$\Lambda = \frac{\lambda n(A_n/A_m)}{n-m} \quad (39)$$

where  $A_n$  is the amplitude of the  $n$ th cycle.  $M$  is taken as the mass of the weights plus that of half of the total (unladen) structure, since the structure was symmetrical about the mid point of the laminates. For tensile axial loads the structure was hung from the top board and weights were placed on the lower board.

On the assumption that only the rubber is responsible for energy dissipation,  $\Lambda$  may be related to  $U_R$  by

$$\Lambda = \pi \tan \delta (U_R / 0.5YW) \quad (40)$$

since the fraction of energy lost on a full cycle (positive and negative shear strains) is  $2\pi \tan \delta$  for low to moderate values of the loss angle  $\delta$ .

The results are compared to the predictions of the theory in Figures 13 and 14.

## 6. DISCUSSION

It has been shown here that provided  $\alpha \lambda$  is sufficiently large then most of the deformation energy is stored in the rubber. It has been shown elsewhere<sup>4</sup> that provided  $\alpha \lambda$  is neither large nor too small the springs can undergo larger deflections than conventional metal leaf springs of the same length, a compromise value of  $\alpha \lambda$  being around 10. It thus appears that the laminated springs have useful characteristics and are, in essence, rubber springs. The sole function of the metal layers is to constrain the deformation of the rubber to be simple shear.

An additional feature of the spring is that by using a multilayer construction, rubbers of different levels of damping can be used together in a parallel deformation. This may allow layers of very high damping elastomer to be used, as analogues to oil-filled dampers, in combination with a layer of highly elastic rubber. Elastomers with very high damping are seldom used in conventional rubber springs because, on their own, they generally suffer from unacceptably high creep. Most conventional rubber springs do not lend themselves to parallel deformation of two separate elastomers.

The effect of axial load on lateral stiffness, stability and damping of the laminar struts is close to that predicted. Considering that there are no fitting parameters available (all parameters having been determined by independent experiments) the agreement may be taken as satisfactory.

Figure 14 suggests that in fact the predicted load for instability is slightly in error, which may be due, for example, to some uncertainty in the rubber modulus. The deviation of the experimental results below the theoretical values for tensile  $P$  may arise from imperfections in the clamping at the ends of the struts, which might progressively come to resemble pin joints as the tension increases. This would act to reduce the lateral stiffness towards  $P/2$ . The theoretical result in Figure 14 can, in fact, be interpreted as the provision by the flexing stiffness of the strut of an almost constant extra lateral stiffness, of magnitude  $Gh/2$ , over and above the axial force term (for a pin-jointed rod) of  $P/2$ .

As the axial load approaches the buckling load the apparent level of damping to horizontal vibrations increases asymptotically. The explanation of this phenomenon is that the apparent damping is determined by the ratio of the energy dissipated in a lateral deflection (of the given magnitude) to the energy required to achieve the deflection. The dissipated energy depends primarily on the deflection and is comparatively insensitive to the axial load (see Figure 10). In particular, the dissipated energy remains finite at the buckling load. However, the energy required to deflect the strut laterally falls towards zero as instability is approached, so that the ratio rises asymptotically.

This phenomenon is quite general, and has been reported previously for conventional laminated rubber bearings.<sup>5,6</sup> Such bearings are used as building mounts to achieve isolation from seismic accelerations. Substantial damping is an essential requirement for base isolation mounts, because some excitation of the natural frequency of the building on the mounts invariably occurs. It appears that enhancement of damping could usefully be contrived by designing the system such that some of the bearings are loaded close to their point of instability. These bearings will make little contribution to the lateral restoring force, but will make a useful contribution to damping.

The sensitivity of the lateral stiffness and the damping to the axial load also has significance for the measurement of material properties. For example, the apparent damping level of a taut strip of rubber undergoing lateral vibrations is much lower than the true level of damping of the material. This phenomenon is exploited to good effect in stringed musical instruments, but may cause some test methods to give misleading results for material properties (Thomas, work to be published).

#### REFERENCES

1. Mead, D. J. and Markus, S., 1969, J. Sound Vib. 10(2), 163-175
2. Muhr, A. H. & Thomas, A. G., paper No.77, Rubber Division meeting of the ACS, Cincinnati, October.
3. Thomas, A.G., 1985, Proc. Int. Rubber Conf., Kuala Lumpur, Malaysia, pages 97-100.
4. Brimblecombe F.A., Muhr, A.H. & Thomas, A.G. 1987, Rubber & Plastics News, August 10th.
5. Thomas, A.G. 1982, Proc. Int. Conf. on Natural Rubber for Earthquake Protection of Buildings and Vibration Isolation, Kuala Lumpur, Malaysia (published MRRDB) pages 1-14.
6. Chan, G.K. & Kelly, J.M., 1987, Report No.UCB/EERC-86/12, Earthquake Engineering Research Center, University of California.
7. Pond, T.J. & Thomas, A.G. 1989, to be published in Journal of Natural Rubber Research.

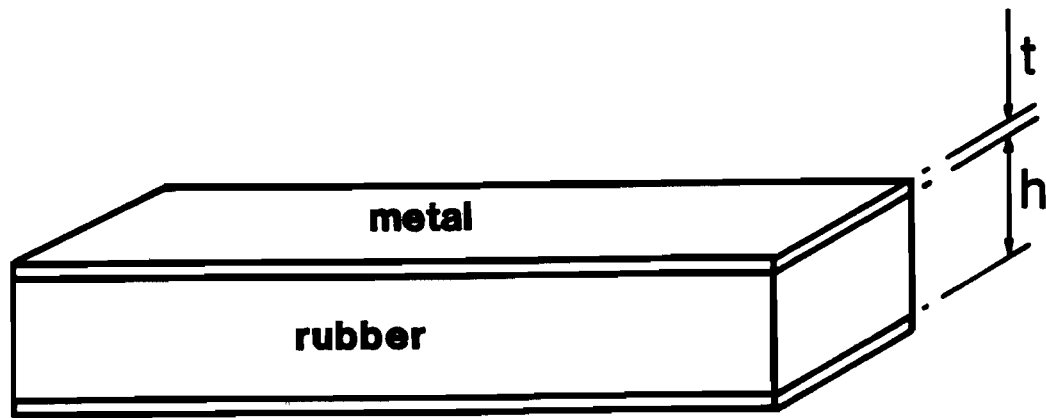


**Figure 1**

Structure of the laminates

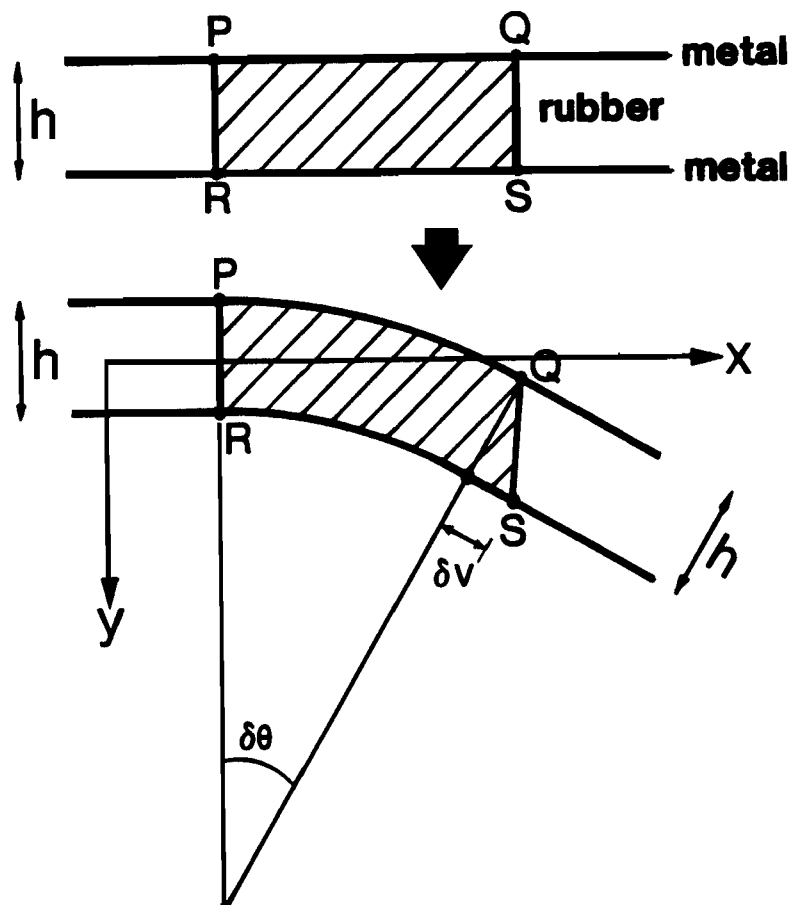


**Figure 2**

Deformation of an element of rubber between thin, inextensible layers of metal

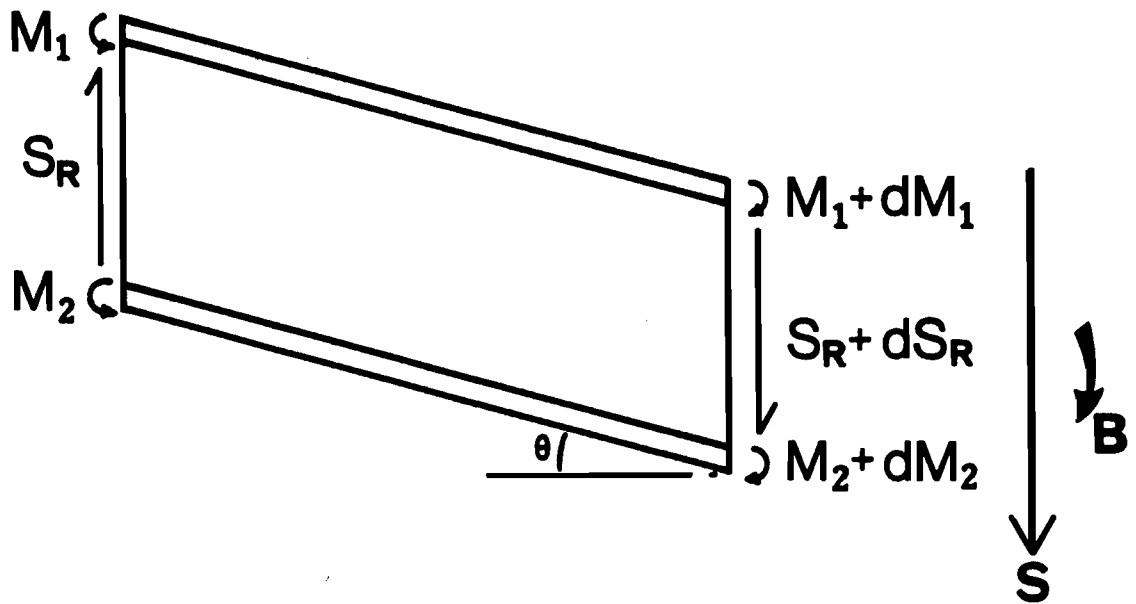


**Figure 3**  
System of forces applied to an element of the laminate.

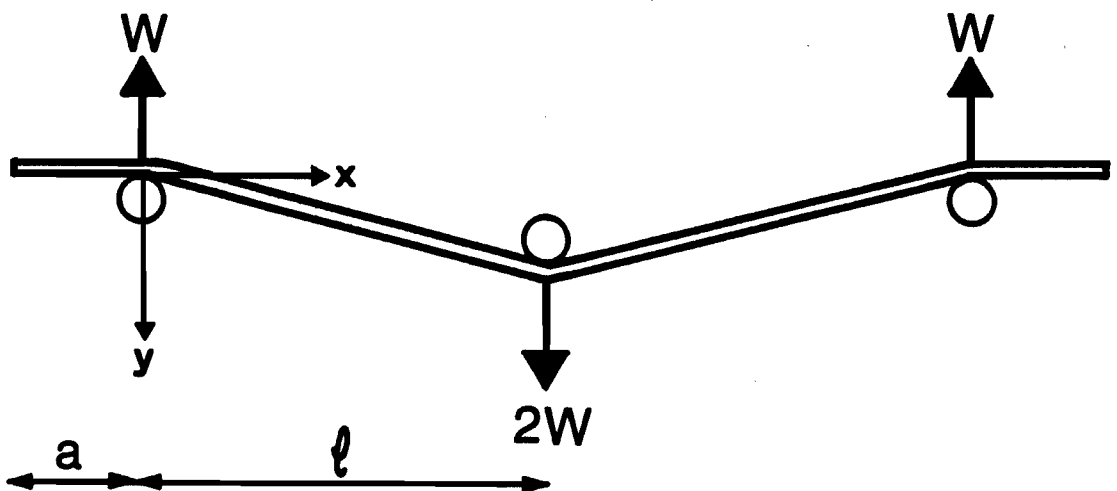


**Figure 4**  
Three point bend geometry.



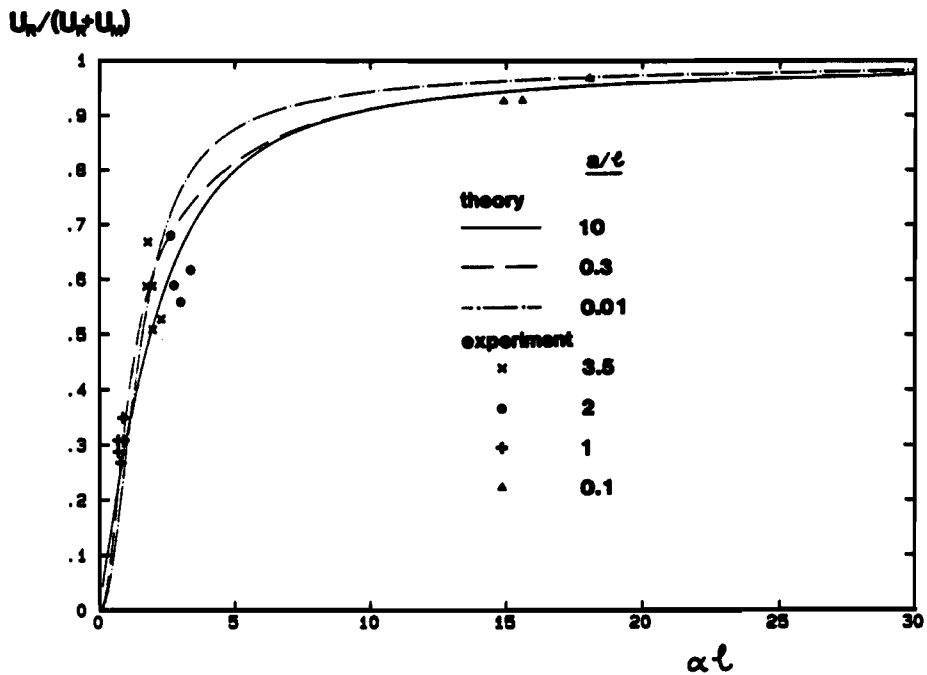


**Figure 5**

Fraction of energy ( $U_R / (U_R + U_M)$ ) stored in the rubber in three point bend deformation as a function of the non-dimensional parameter  $\alpha l = \sqrt{Gh/R\lambda}$

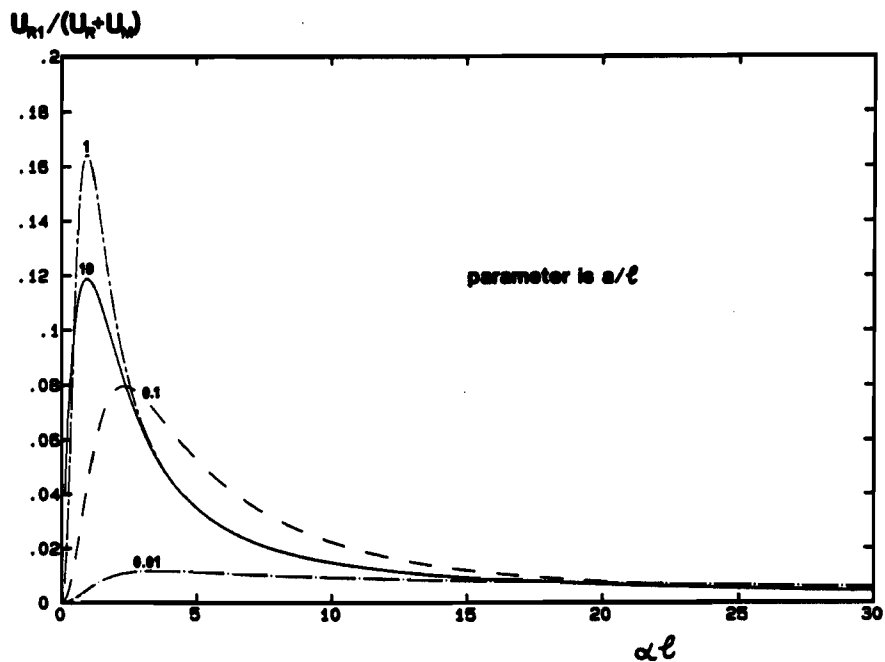


**Figure 6**

Fraction of energy ( $U_{R1} / (U_R + U_M)$ ) stored in the rubber in the overhang for the three point bend deformation

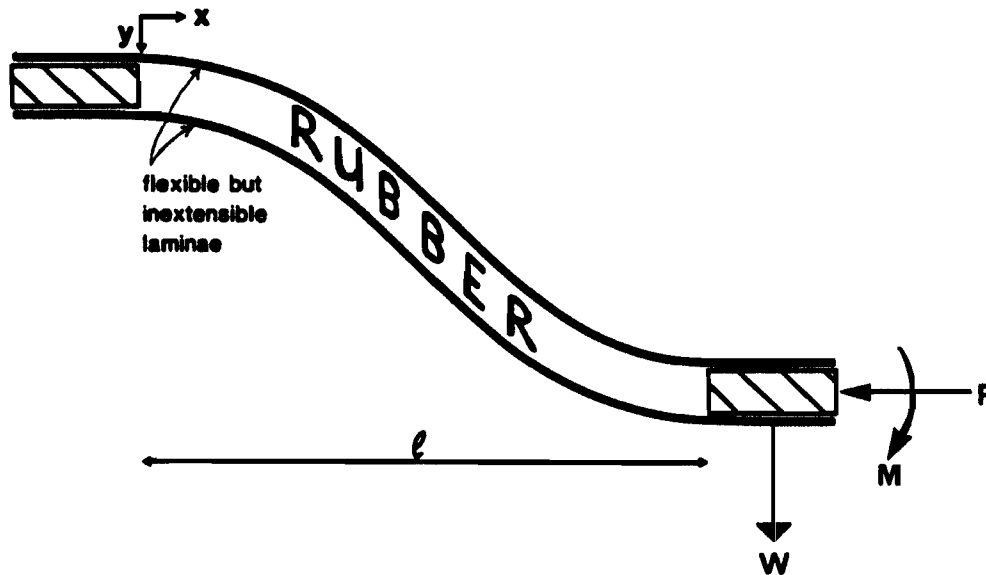


**Figure 7**

Laminar strut geometry (note that the metal layers are interconnected at the ends).

$(W/Y)(l/Gh)$

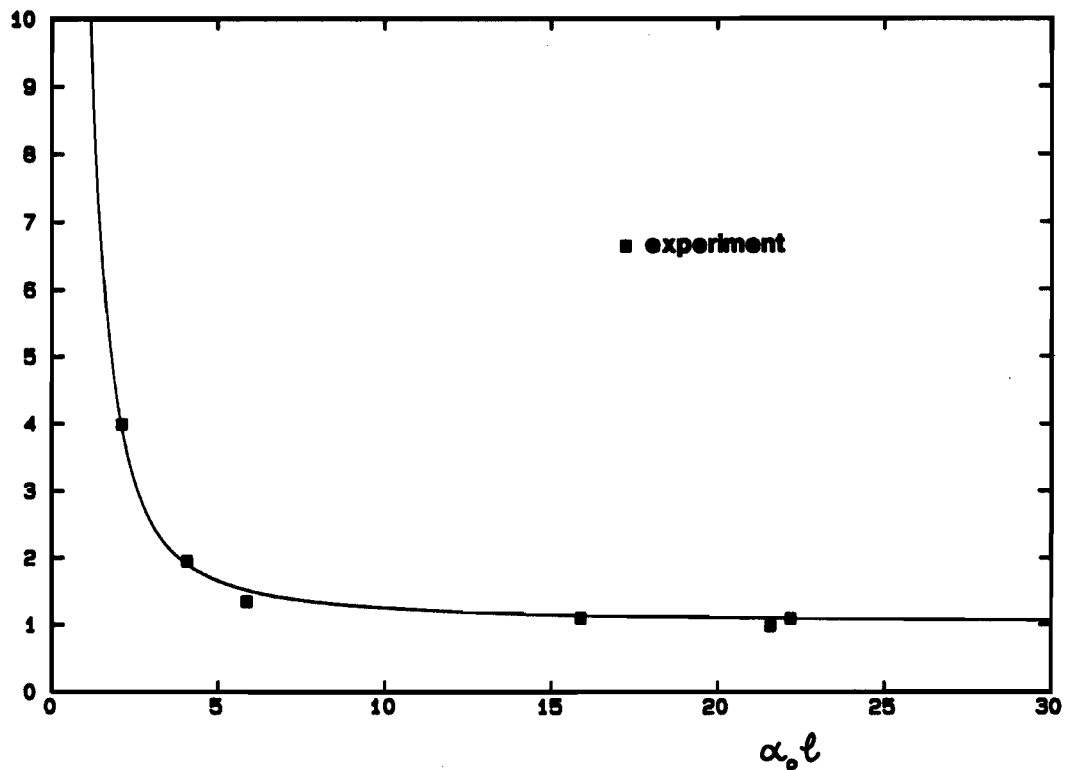


**Figure 8**

Lateral stiffness of laminar strut (with zero axial load) versus the non-dimensional parameter  $\alpha_0 l$  (equal to  $\sqrt{Gh/K\kappa}$ )

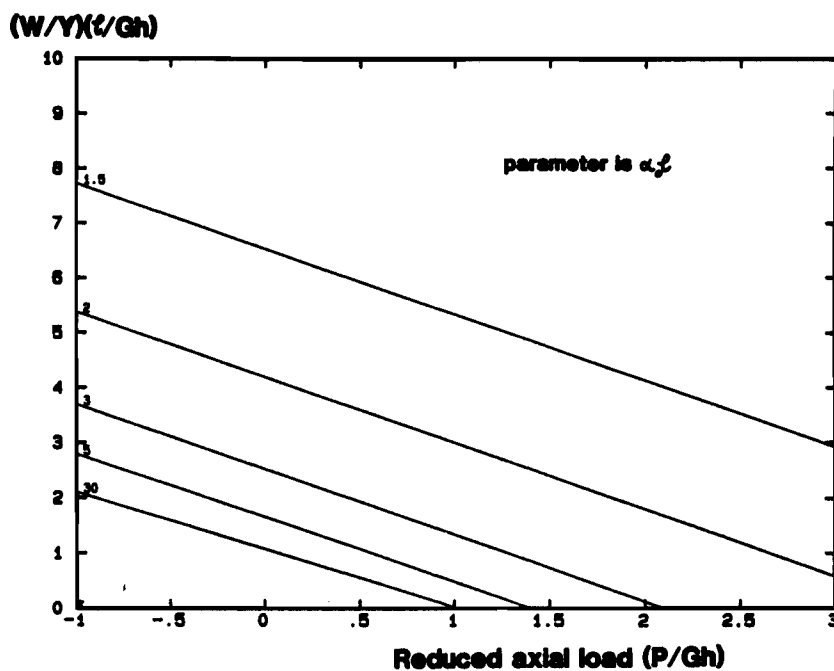


**Figure 9**

Effect of axial load P on the lateral stiffness of laminar struts

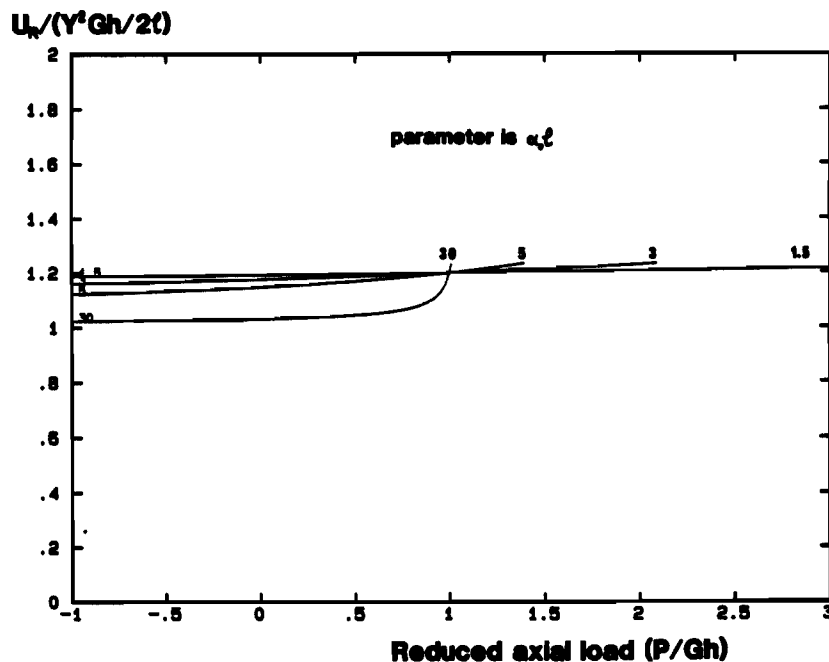


**Figure 10**

Effect of axial load P on the energy stored in the rubber for a laminar strut (at unit lateral deflection)

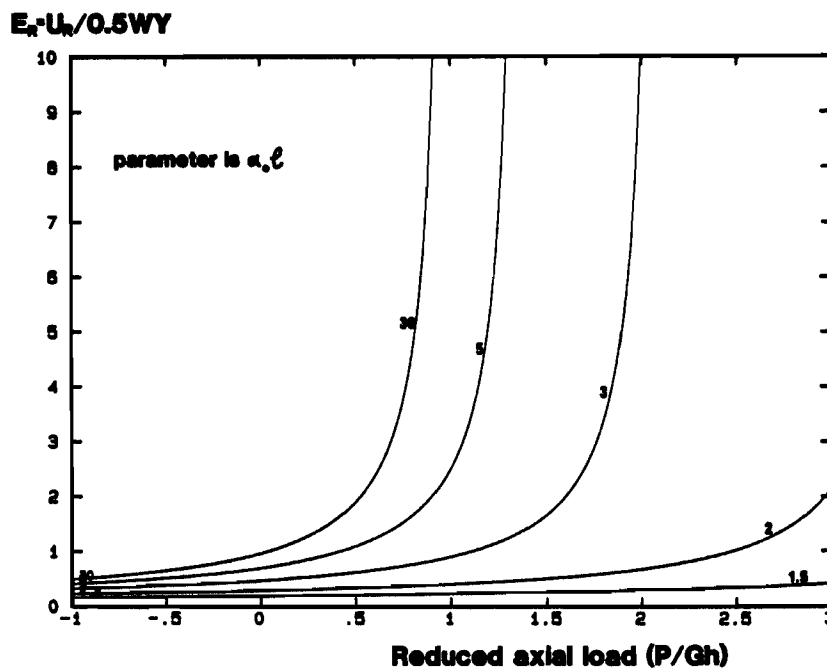


Figure 11

Effect of axial load  $P$  on the damping of lateral oscillations of laminar struts

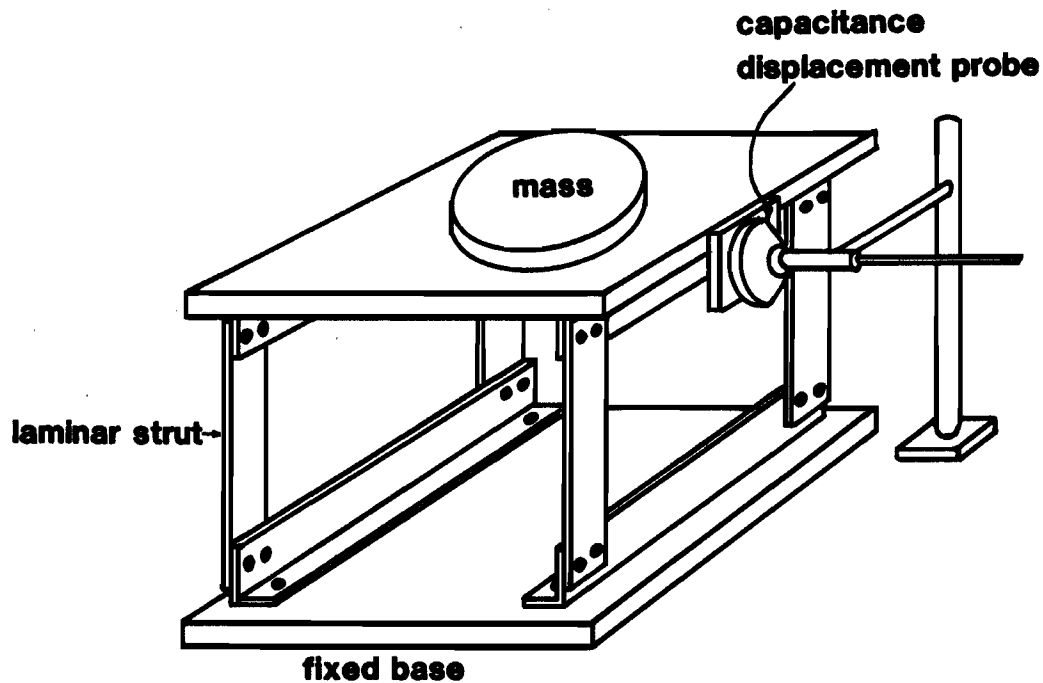


Figure 12

Arrangement for measuring the effect of axial load on the lateral stiffness and damping of laminar struts

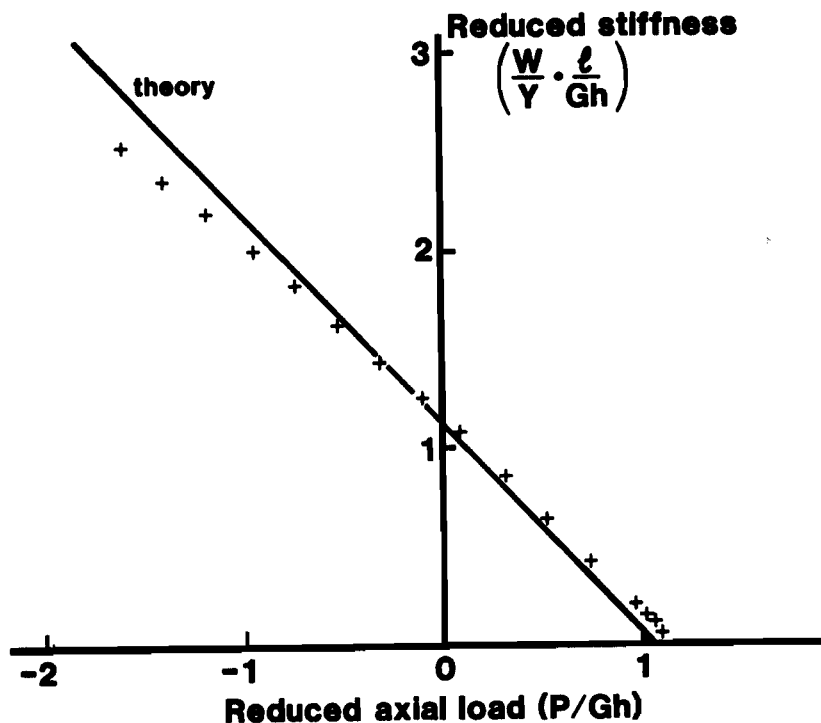


Figure 13

Experimental check of the effect of axial load (P) on the stiffness of laminar struts

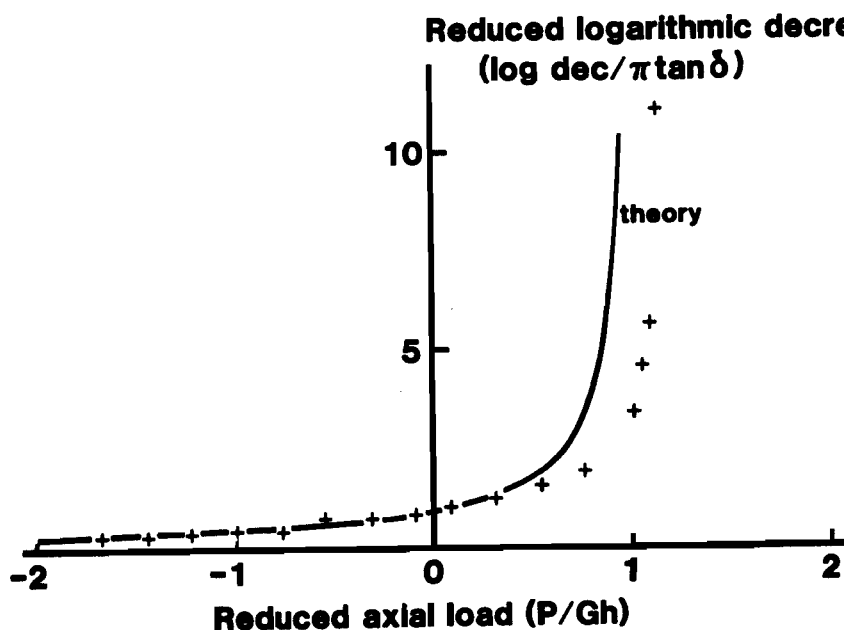


Figure 14

Experimental check of the effect of axial load (P) on the logarithmic decrement of lateral oscillations of laminar struts